



HAL
open science

Numerical Investigations of the Thermal, Pressure and Size Effects on 2D Spin Crossover Nanoparticles

Camille Harlé, Salah Eddine Allal, Devan Sohier, Thomas Dufaud, R. Caballero, F. de Zela, Pierre-Richard Dahoo, K. Boukheddaden, Jorge Linares

► **To cite this version:**

Camille Harlé, Salah Eddine Allal, Devan Sohier, Thomas Dufaud, R. Caballero, et al.. Numerical Investigations of the Thermal, Pressure and Size Effects on 2D Spin Crossover Nanoparticles. *Journal of Physics: Conference Series*, 2017, 936, pp.012061. 10.1088/1742-6596/936/1/012061 . insu-01576253

HAL Id: insu-01576253

<https://insu.hal.science/insu-01576253v1>

Submitted on 26 Jan 2018

HAL is a multi-disciplinary open access archive for the deposit and dissemination of scientific research documents, whether they are published or not. The documents may come from teaching and research institutions in France or abroad, or from public or private research centers.

L'archive ouverte pluridisciplinaire **HAL**, est destinée au dépôt et à la diffusion de documents scientifiques de niveau recherche, publiés ou non, émanant des établissements d'enseignement et de recherche français ou étrangers, des laboratoires publics ou privés.

PAPER • OPEN ACCESS

Numerical Investigations of the Thermal, Pressure and Size Effects on 2D Spin Crossover Nanoparticles

To cite this article: C. Harlé *et al* 2017 *J. Phys.: Conf. Ser.* **936** 012061

View the [article online](#) for updates and enhancements.

Numerical Investigations of the Thermal, Pressure and Size Effects on 2D Spin Crossover Nanoparticles

C. Harlé¹, S.E. Allal¹, D. Sohier², T. Dufaud^{2,3}, R. Caballero⁴, F. de Zela⁴, P. R. Dahoo¹, K. Boukheddaden⁵, J. Linares^{4,5}

¹LATMOS, Université de Versailles-Saint-Quentin-en-Yvelines, CNRS-UPMC-UVSQ (UMR 8190), 11 boulevard d'Alembert, 78280 Guyancourt, France

²LI-PaRAD, Université de Versailles Saint-Quentin-en-Yvelines, 45 Av. des Etats-Unis, EA 7432, 78035 Versailles Cedex, France

³Maison de la Simulation, Université de Versailles Saint-Quentin-en-Yvelines, CNRS - USR 3441, Bâtiment 565 - Digiteo CEA Saclay, 91191 Gif-sur-Yvette cedex, France

⁴Departamento de Ciencias, Sección Física, Pontificia Universidad Católica del Perú, Apartado 1761 - Lima, Peru

⁵GEMAC, Université de Versailles Saint-Quentin-en-Yvelines, 45 Av. des Etats-Unis, CNRS-UMR 8635, 78035 Versailles Cedex, France

Abstract: In the framework of the Ising-like model, the thermal and pressure effects on the spin crossover systems are evaluated through two-states fictitious spin operators σ with eigenvalues $\sigma = -1$ and $\sigma = +1$ respectively associated with the low-spin (LS) and high-spin (HS) states of each spin-crossover (SCO) molecule. Based on each configurational state, the macroscopic SCO system, is described by the following variables: $m = \sum \sigma$, $s = \sum \sigma_i \sigma_j$ and $c = \sum \sigma_i$, standing respectively for the total magnetization, the short-range correlations and surface magnetization. To solve this problem, we first determine the density of macrostates $d[m][s][c]$, giving the number of microscopic configurations with the same m , s and c values. In this contribution, two different ways have been performed to calculate this important quantity: (i) the entropic sampling method, based on Monte Carlo simulations and (ii) a new algorithm based on specific dynamic programming. These two methods were tested on the 2D SCO nanoparticles for which, we calculated the average magnetization $\langle \sigma \rangle$ taking into account for short-, long-range interactions as well as for the interaction between surface molecules with their surrounding matrix. We monitored the effect of the pressure, temperature and size on the properties of the SCO nanoparticles.

1. Introduction

Spin transition compounds are part of inorganic coordination complexes of transition metal ions with $3d^4$ - $3d^7$ electron configurations, namely Fe(II), Fe(III), Co(II), Mn(II), and Ni(II), located in an octahedral ligand field, the strength of which induces the competition between spin states^[1-9]. These compounds are usually known as bistable materials, are able to switch between the diamagnetic low-spin state (LS), stable at low-temperature, and the paramagnetic high spin-state (HS), stable state at high-temperature, due to its larger entropy. Due to the local volume change accompanying each spin transition of the molecules, long- and short-range range elastic interactions^[10-13] take place between the SCO units causing cooperative hysteretic first-order thermal transitions, driven by the large entropy (originating from spin and vibrations) of the HS state compared to that of the LS. In addition to the temperature^[1-2], the spin state can also be switched by the application of pressure^[14-17], by a magnetic



field^[18], or by an irradiation in the visible light^[19]. In this work, we will focus exclusively on thermal and pressure effects. From the experimental side, the switching between the LS and HS states results in large changes in magnetic, optical, and dielectric properties of SCO compounds, which make them potential candidates as promising nano-materials for innovative applications such as ultra-sensitive sensors, in data storage or as display devices. From the theoretical side, the modelling of SCO phenomena helps to get new insights on the physical properties of SCO nanoparticles, particularly those displaying phase transitions, whose behaviour as function of their size and their interaction parameters play an important role in the control of the switching features of these complex materials, with the ultimate goal to help to design novel ones with specific ones with tailored properties.

Furthermore, the modelling of phase transitions makes possible the understanding of the intimate processes of cooperativity in SCO solids, and how these interactions between molecules are influenced by the various constraints applied to the material, like light, pressure or temperature. On the other hand, it is now widely admitted that long range interactions between SCO molecules are of elastic origin and that depending on their strength compared to the ligand field energy, the high spin fraction curve can display different shapes, whose features can change gradually, abruptly, or in two-step with or without hysteresis. In SCO nanoparticles, these trends are intrinsically related to the cooperativity between the SCO units but also to the size of the nanoparticles as well as to other external constraints influencing the transition, as it will be demonstrated in the present work.

The manuscript is organized as follows: section (2) devoted to the presentation of the model Hamiltonian, then to the methods of resolution and finally to the results of the numerical simulations conducted on the 2D lattices. The discussion of the behaviour of the high-spin fraction obtained using several stimuli will be realized in this section. In section (3) we conclude and outline some possible extensions of the present work.

2. Results and discussion

The different simulations we have carried out in the present investigations were based on the Ising-like model^[20-22], in which we analysed the behaviour of the average net magnetization $\langle \sigma \rangle$ or HS fraction, $N_{HS} = \frac{1+\langle \sigma \rangle}{2}$, that is to say the probability of obtaining of HS molecules in the material under study. We have considered the following lattice configurations of size: 4x4 and 12x12 in 2D, and 1x12 and 1x500 for the 1D case.

To deeply explore the thermal and pressure properties of SCO nanoparticles, we simulated N_{HS} as a function of temperature and pressure thanks to various parameters such as: (i) the ligand-field Δ which represents the energy gap between the LS and HS states of isolated spin-crossover units, (ii) the respective short- and long-range interaction parameters, J and G , (iii) the interaction between the molecules at the surface and their environments, L , introduced by Linares *et al*^[23-24], (iv) $\ln(g)$ with $g = g_{HS} / g_{LS}$ corresponding to the ratio of degeneracies of the 2 spin states.

The specific Ising-like designed to mimic the SCO nanoparticles under various constraints writes under the following form^[15-16]:

$$H = \frac{\Delta + \Delta V.P}{2} - k_B T \ln g \sum_{i=1}^N \sigma_i - G \sum_{i=1}^N \sigma_i \langle \sigma \rangle - J \sum_{\langle i,j \rangle} \sigma_i \sigma_j - L \sum_{i=1}^M \sigma_i \quad (1)$$

Hamiltonian (1) has the advantage to make possible to simulate the material's behaviour in an environment that is characterized by interactions that occur not only in the core of the material, but also at the edge.

The first term in (1) results from one site contributions and concerns all lattice atoms, the second term accounts for long-range interactions and it is written here under the form a mean-field in which $\langle \sigma \rangle$

is the average magnetization per site. The third term expresses short-range interactions between the SCO species, while the last term only acts on surface molecules due to their specific environment.

In addition, Hamiltonian (1) includes the contribution of an external isotropic pressure, whose effect is to renormalize the ligand field energy, the effective expression of which becomes, $\Delta + \Delta V.P$, where P is the applied external pressure and $\Delta V = V_{HS} - V_{LS}$ is the volume change of the material between the HS and the LS states. Here, N is the total number of molecules in the lattice and M the number of molecules at the surface ("edge").

The following macroscopic parameters will be useful in the description of the thermodynamic properties:

$$m = \sum_{i=1}^N \sigma_i \quad s = \sum_{\langle i,j \rangle} \sigma_i \sigma_j \quad c = \sum_{k=1}^M \sigma'_k \quad (2)$$

Where σ'_k represents the molecules on the edge. There, m and c are the total and surface magnetizations, s is the sum of two spins correlations in the lattice.

Then the Hamiltonian can be cast as:

$$H = \left(\frac{\Delta + \Delta V.P - k_B T \ln g}{2} - G \langle \sigma \rangle \right) m - Js - Lc \quad (3)$$

where, $\frac{m}{N} = \langle \sigma \rangle$. Eq. (3) clearly indicates that the knowledge of the density of states $d(m, s, c)$, that represents the number configuration with the same m , s and c values, allows the determination of all thermodynamic properties of this system.

The average value of operator σ is given by:

$$\langle \sigma \rangle = \frac{\sum_{i=1}^{NL} \frac{m_i}{N} d(m_i s_i c_i) \exp \left(-\frac{1}{k_B T} (-hm_i - Js_i - Lc_i) \right)}{\sum_{i=1}^{NL} d(m_i s_i c_i) \exp \left(-\frac{1}{k_B T} (-hm_i - Js_i - Lc_i) \right)} \quad (4)$$

where NL is the number of possible configurations $\{m, s, c\}$, and h is expressed as :

$$h = - \left(\frac{\Delta + \Delta V.P - k_B T \ln g}{2} - G \langle \sigma \rangle \right) \quad (5)$$

The density of macrostates, $d(m, s, c)$, and the different configurations $\{m, s, c\}$, have been calculated using Monte Carlo Entropic Sampling^[25] and also by a new dynamic programming algorithm.

Now we introduce the assumption that the transition temperature of the system is the result of a null total effective ligand-field. So, the transition temperature, T_{eq} , for a square lattice $N_x \times N_x$ is the solution of the following equation:

$$\frac{\Delta + \Delta V.P - k_B T_{eq} \ln g}{2} \times (N_x - 2)^2 + \frac{\Delta + \Delta V.P - 2L - k_B T_{eq} \ln g}{2} \times 4(N_x - 1) = 0 \quad (6)$$

where, $(N_x - 2)^2$ and $4(N_x - 1)$ are respectively the number of the core and the edges sites. Solving this linear equation gives the analytical expression of transition temperature as function of the lattice size and the bulk, T_{eq}^{bulk} , and surface, T_{eq}^{surf} , transition temperatures:

$$T_{eq} = \frac{N_c}{N} T_{eq}^{bulk} + \frac{N_s}{N} T_{eq}^{surf} \quad (7)$$

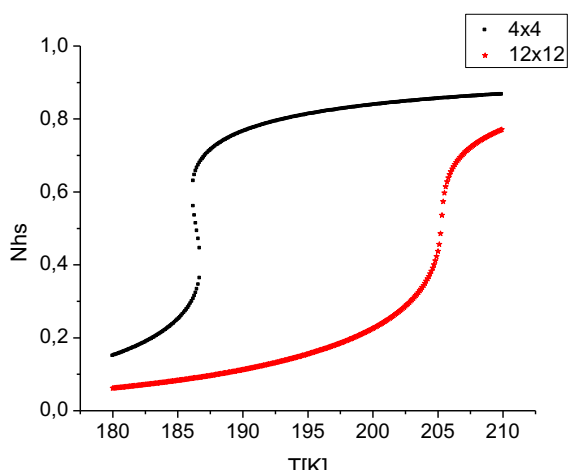
where the analytical expressions of the transition temperatures associated to the bulk and the surface, are:

$$T_{eq}^{bulk} = \frac{\Delta + \Delta V \cdot P}{k_B \ln g} \text{ and } T_{eq}^{surf} = \frac{\Delta + \Delta V \cdot P - 2L}{k_B \ln g} \quad (8)$$

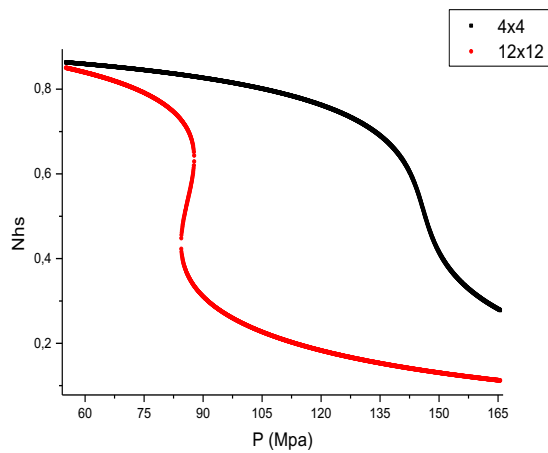
The present investigations are mainly focussed on the role of the interaction between the matrix and the molecules at the surface, i.e. L (which is one of the most relevant parameters is the behaviour of SCO nanoparticles) on the thermal properties of SCO nanoparticles. At this end, we simulate the thermal behaviour of SCO system in isobaric conditions as well as its pressure dependence in isothermal conditions, for $L=0$ and $L \neq 0$.

The 2D case:

We first start with the situation $L \neq 0$. The results of the dynamic algorithm programming leading to the exact density of states, from which we derived the thermodynamic properties of the studied lattices, are presented in Fig 1, which summarizes the temperature dependence of the HS fraction for a fixed pressure value. For the parameter values, $\Delta/k_B = 1300$ K, $G/k_B = 172.2$ K, $J/k_B = 13.5$ K, $L/k_B = 120$ K, $\ln(g) = 6.01$, we clearly see that the square lattice 12×12 does not show any thermal hysteresis. In contrast, when the lattice's size is reduced to a 4×4 , a thermal hysteresis appears. To understand this trend, one has to analyse carefully the role of surface effects. In fact, by decreasing the lattice's size, the surface effects become dominant, the transition temperature approaches that of the surface, $(\Delta - 2L)/k_B \ln(g) \sim 176$ K. To see whether, the first order transition occurs or not at the surface, it is important to evaluate the order-disorder transition, T_{OD} , of the system under short- and long-range interactions J and G , for $\Delta=0$, $L=0$ and $g=1$. In the case $J=0$, the order-disorder transition is equal to that of the mean-field model $T_{OD}=G/k_B$, while in the case $G=0$ and $J \neq 0$, the order-disorder is given by the exact Onsager's expression, $T_c=2.269J=30,63$ K. When the short- and long-range interactions are nonzero, the transition order-disorder transition can be approximately estimated to $T_c = (2.269J+G)/k_B \sim 203$ K, a value in quite good agreement with that found by our numerical simulations on the same system. Compared to the previous value of T_c (203 K), we have $T_{eq}^{surf} (\sim 176 \text{ K}) < T_c$, while T_{eq}^{bulk}



($=216$ K) $> T_c$. The latter conditions lead to a gradual transition, while the former implies the existence of a thermal hysteresis. So decreasing the size, enhances the surface effects for which the conditions of appearance of first-order transition are fulfilled.



(1)

(2)

Figure 1. Thermal evolution of the high spin fraction for the two lattice sizes: 4x4 (black square) and 12x12 (red star). The parameters value are: $\Delta/k_B = 1300$ K, $G/k_B = 172.2$ K, $J/k_B = 13.5$ K, $L/k_B = 120$ K, $\ln(g) = 6.01$.

Figure 2. Evolution of the high spin fraction versus the pressure for 2 sizes: 4x4 (black square) and 12x12 (red circle); the parameters value are: $\Delta/k_B = 1978.6$ K, $G/k_B = 172.2$ K, $J/k_B = 48$ K, $L/k_B = 120$ K, $T = 300$ K, $\ln(g) = 6.906$, $\Delta V = 100 \text{ \AA}^3$.

Now, we inspect the effect of a hydrostatic pressure on the thermal properties of the SCO material. According to Eq. (8), we can easily see that pressure appears a conjugate parameter of temperature. Under pressure, the transition temperature of the SCO lattice increases as a result of the increase of the ligand field, which stabilizes the LS state, which has a smaller volume, compared to that of the HS state. Thus, increasing pressure is somehow equivalent to reduce temperature, which leads to switch the SCO system between the HS and the LS states.

Thus, once again, as seen in Fig. 2, the thermal behaviour and the pressure behaviour are reversed concerning the hysteresis since the system switches from the HS to the LS state by increasing pressure. Although not discussed, this isothermal transition crucially depends on temperature, whose variation affects the width of the pressure hysteresis and even the character (first-order or gradual) of the transition.

The case $L=0$:

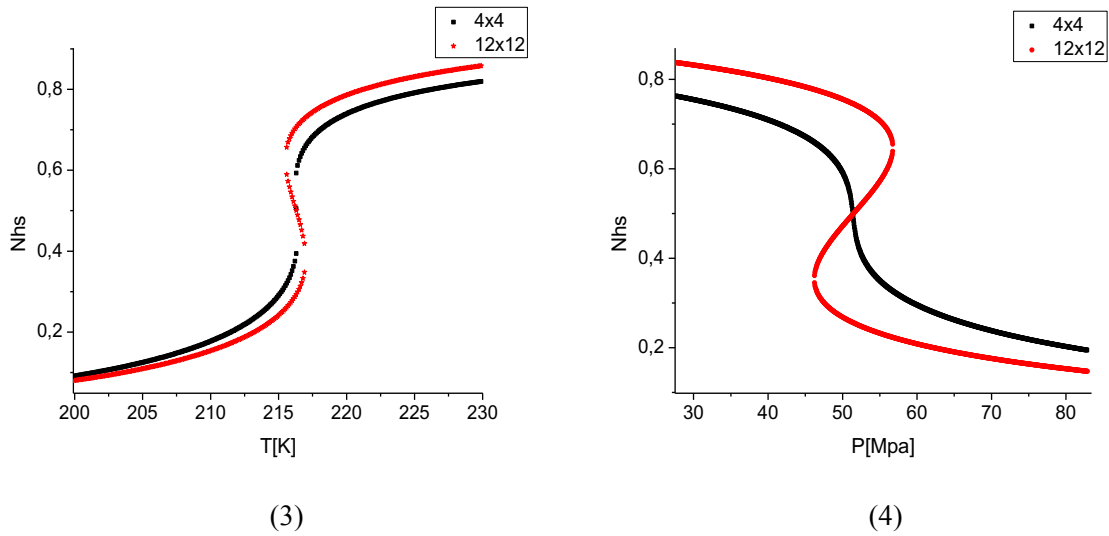


Figure 3. Thermal evolution of the high spin for two lattice sizes: 4x4 (black square) and 12x12 (red star) at zero applied pressure. The parameters value are: $\Delta/k_B = 1300$ K, $G/k_B = 172.2$ K, $J/k_B = 16.8$ K, $L/k_B = 0$ K, $\ln(g) = 6.01$.

Figure 4. Pressure-dependence of the HS fraction in isothermal conditions ($T=300$ K) for two lattice sizes: 4x4 (black square) and 12x12 (red circle). The parameters value are: $\Delta/k_B = 1978.6$ K, $G/k_B = 172.2$ K, $J/k_B = 48$, $L/k_B = 0$ K and $\ln(g) = 6.906$.

Unlike the case $L \neq 0$, we note that the behaviour is almost identical: the hysteresis width increases when the size is increased. Moreover, it can be noticed for the thermal behaviour that the equilibrium temperature which corresponds to $N_{hs} = \frac{1}{2}$ is the same whatever the size of the material. Indeed, when $L=0$ is set, the lattice does not experience any surface effects and consequently, according to Eqs. (7) and (8), the transition temperature, T_{eq} , remains independent on the lattice size. In contrast, the order-disorder transition T_{OD} (obtained for $\Delta = 0$ and $g=1$) increases with lattice size, which clearly explains the reason for which the thermal hysteresis becomes wider (see Fig. 3) as the lattice size increases.

Applying an isotropic pressure on the system, in isothermal conditions at $T=300$ K, results in the pressure hysteresis of Fig. 4. Interestingly, the latter is much wider than that of Fig. 2 with a pressure hysteresis width equal to $\Delta P \sim 13$ MPa against 7 MPa for Fig. 2 and a pressure transition $P_{1/2}^{bulk} = (k_B T \ln(g) - \Delta) / \Delta V \sim 52$ MPa, which is smaller than that of Fig. 2 which is affected by the surface effects.

3. Conclusion

In this paper, we analysed the thermal and pressure behaviour of 1D and 2D spin-crossover compounds with particular attention paid to the effect of the interactions between molecules at the edges of the nanoparticles and their local environment, which were taken into account in the coupling parameter, L . When $L = 0$, the thermal and pressure behaviour are identical and the increase in size is characterized by the appearance of a hysteresis. However, for L different from zero, the behaviours due to the applied pressure and the temperature are reversed with respect to the modification of the size of the material. This result, which is directly linked to the thermal behaviour, as the only property that is reversed when L is modified, is explained by a quantitative relationship between the equilibrium temperature and the order-disorder temperature of the same Hamiltonian with a degeneracy ratio $g=1$ and without ligand field, i.e. $\Delta=0$ and $L=0$. Differently, we observed that the effect of pressure does not depend significantly on L , except for the very small sizes. Indeed, the effect of pressure combines both surface and bulk effects and so its impact on the surface depends on the

ration surface/volume. Moreover, since the ligand field at the surface of the lattice is weaker than that of the bulk, due to matrix's contribution, the effect of pressure will be clearly different on the surface and the volume. Furthermore, the elastic properties of the material are different in the surface and the volume^[12-13] as well as the phonon spectra, which may constitute an interesting target for future investigations. In addition, one may underline the fact the interaction parameters (J and G) themselves may depend on the applied pressure, since the latter are elastic in nature and then should be influenced by the change of the elastic constants under high pressure, for example. This interesting point will be also investigated in a near future, by adopting simple expansions of the interaction parameters with the applied pressure. Despite of these possible extensions, the effect of the various factors, such as the internal interaction strength, the local environment or the system's size, on the thermal and pressure induced transition, reported in the present work, are consistent with several experimental findings in this area. As underlined, the current work opens the way to many interesting extensions which will be helpful for a deeper understanding of the SCO properties under various stimuli, which are mandatory prerequisites for the development of new technological applications based on the switchable properties of these materials.

Acknowledgments

CHAIR Materials Simulation and Engineering, UVSQ, Université Paris Saclay is gratefully acknowledged. The present work has also been supported by the French "Ministère de la Recherche", Université de Versailles St. Quentin en Yvelines, CNRS and ANR BISTA-MAT: ANR-12-BS07-0030-01, whose support is highly appreciated.

References

- [1] Hauser A., *Coord. Chem. Rev.*, 111, 275-290, (1991)
- [2] Gütllich P, Gaspar AB and Garcia Y, *Beilstein J. Org. Chem.* 9 342, (2013)
- [3] Varret F., Bleuzen A., Boukheddaden K., Bousseksou A., Codjovi E., Enachescu C., Goujon A., Linares J., N. Menendez N. and M. Verdaguer M., *Pure Appl. Chem.*, 74, 2159-2168, (2002)
- [4] Sy M. , Garrot D., Slimani A., Paez-Espejo M., Varret F., Boukheddaden K., *Ang. Chem*, 128, 1787-1791, (2016)
- [5] Enachescu C., Linares J. , Varret F. , *J. Phys.:Condens. Matter*, 13,2481-2495, (2001)
- [6] Jureschi C., Linares J., Boulmaali A., Dahoo P.R., Rotaru A. and Garcia Y., *Sensors*,16, 187, (2016)
- [7] Seredyuk M, Gaspar AB, Ksenofontov V, Reiman S, Galyametdinov Y, Haase W, Rentschler E, Gütllich P, *Chem. Mater.* 18 2513, (2006)
- [8] Mishra V., Mukherjee R., Linares J., Balde C., Desplanches C., Létard J.F., Collet E., Toupet L., Castro M., Varret F. , *Inorg Chemistry*, 47, 7577-7587, (2008)
- [9] Kamel Boukheddaden, Isidor Shteto, Benoit Hôo, and François Varret, *Phys. Rev. B* 62, 14796, (2000)
- [10] Ahmed Slimani, Kamel Boukheddaden, François Varret, Hassane Oubouchou, Masamichi Nishino, and Seiji Miyashita, *Phys. Rev. B* 87, 014111, (2013)
- [11] Miguel Paez-Espejo, Mouhamadou Sy, and Kamel Boukheddaden, *J. Am. Chem. Soc.*, 138, 3202–3210, (2016)
- [12] Kamel Boukheddaden, *Phys. Rev. B* 88, 134105, (2013)
- [13] Masamichi Nishino, Kamel Boukheddaden, and Seiji Miyashita, *Phys. Rev. B* 79, 012409, (2009)

- [14] Klokishner S., Linares J., Varret F., *Chemical. Physics*, 255, 317-323, (2000)
- [15] Morscheidt W, Jeftic J, Codjovi E, Linares J, Bousseksou A, Constant-Machado H, Varret F, *Meas. Sci. Techn.*, 9, 1311-1315, (1998)
- [16] Rotaru A, Varret F, Gîndulescu A, Linares J, Stancu A, Létard JF, Forestier T, Etrillard C, *Eur. Phys. J. B* 84, 439-449, (2011)
- [17] Jeftic J, Menéndez N, Wack A, Codjovi E, Linares J, Goujon A, Hamel G, Klotz S, Syfosse G, Varret F, *Meas. Sci. Techn.*, 10, 1059-1064, (1999)
- [18] Bonhommeau, S.; Molnar, G.; Galet, A.; Zwick, A.; Real, J.A.; McGarvey, J.J.; Bousseksou, A. *Angew. Chem. Int. Edit.*, 44, 4069–4073, (2005)
- [19] Bousseksou, A.; Boukheddaden, K.; Goiran, M.; Consejo, C.; Boillot, M.L.; Tuchagues, J.P. *Phys. Rev. B*, 65, (2002)
- [20] Wajnflasz J, Pick R, *J. Phys. Colloques*, 32, 91-92, (1971)
- [21] Bousseksou A, Nasser J, Linares J, Boukheddaden K, Varret F, *J. Physique I* 2 1381, (1992)
- [22] J. Linares, J. Nasser, A. Bousseksou, K. Boukheddaden, , F. Varret, *J. Mag. Mat.* 140-144, 1503-1504, (1995)
- [23] Linares J, Jureschi C, Boukheddaden K, *Magnetochemistry*, 2, 24, (2016)
- [24] Linares J, Jureschi C, Boulmaali A, Boukheddaden K, *Physica B*, 486, 164–168, (2016)
- [25] Shteto I., Linares J., Varret F., *Physical Review E* 56, 5128-5137, (1997)